

University of Wollongong

## Research Online

---

Faculty of Engineering and Information  
Sciences - Papers: Part A

Faculty of Engineering and Information  
Sciences

---

1-1-2013

### Blast furnace hearth refractory and coke ash mineral interactions

P B. Drain

*University of Wollongong*, pbd150@uowmail.edu.au

M W. Chapman

*BlueScope Steel*, mchapman@uow.edu.au

R J. Nightingale

*University of Wollongong*, robertn@uow.edu.au

B J. Monaghan

*University of Wollongong*, monaghan@uow.edu.au

Follow this and additional works at: <https://ro.uow.edu.au/eispapers>



Part of the [Engineering Commons](#), and the [Science and Technology Studies Commons](#)

---

Research Online is the open access institutional repository for the University of Wollongong. For further information contact the UOW Library: [research-pubs@uow.edu.au](mailto:research-pubs@uow.edu.au)

---

## Blast furnace hearth refractory and coke ash mineral interactions

### Abstract

In the blast furnace hearth the calcium aluminate by-products of coke dissolution can react with the hearth refractories. Reactions between these coke ash minerals and the aluminosilicate and alumina-carbon hearth refractories may result in increased refractory wear reducing the blast furnace campaign life. Hence improved understanding of these interactions may have implications for the campaign life of the blast furnace hearth refractory materials. The interactions between the coke ash minerals and aluminosilicate hearth refractory have been assessed by heating samples of calcium aluminates (CA, CA2 & CA6) coupled with aluminosilicate refractory to temperatures representative of the blast furnace hearth (1450 degrees C to 1550 degrees C) in an inert atmosphere over a range of reaction times (4 - 24 hours). It was found that there was significant reaction between the refractory, CA and CA2 but little reaction with the CA6. The reaction layers formed at the interface between the couples were found to consist of CA2, CA6, corundum, plagioclase and melilite. The formation of a layer with these phases is likely to cause refractory wear due to reduced mechanical strength at highest operating temperatures and by spalling induced by volume changes and changes in thermal expansion characteristics. From assessment of the kinetics of the system it was found that the aluminosilicate refractory followed the linear rate law for reactions with CA and CA2. Given the lack of reaction of the refractory with CA6 little comment can be made on the kinetics other than they are slow.

### Keywords

mineral, ash, interactions, coke, furnace, blast, refractory, hearth

### Disciplines

Engineering | Science and Technology Studies

### Publication Details

Drain, P. B., Chapman, M. W., Nightingale, R. J. & Monaghan, B. J. (2013). Blast furnace hearth refractory and coke ash mineral interactions. *Chemeca 2013: challenging tomorrow* (pp. 270-277). Brisbane, Australia: Institution of Engineers Australia.

# Blast Furnace Hearth Refractory and Coke Ash Mineral Interactions

P.B. Drain<sup>1</sup>, M.W. Chapman<sup>2</sup>, R. J. Nightingale<sup>1</sup>, B. J. Monaghan<sup>1</sup>

<sup>1</sup> University of Wollongong, PYROmetallurgical Group

PO Box 1854, Wollongong, NSW 2500

<sup>2</sup> BlueScope Steel, Ironmaking Technology

[pbd150@uowmail.edu.au](mailto:pbd150@uowmail.edu.au)

## ABSTRACT

In the blast furnace hearth the calcium aluminate by-products of coke dissolution can react with the hearth refractories. Reactions between these coke ash minerals and the aluminosilicate and alumina-carbon hearth refractories may result in increased refractory wear reducing the blast furnace campaign life. Hence improved understanding of these interactions may have implications for the campaign life of the blast furnace hearth refractory materials.

The interactions between the coke ash minerals and aluminosilicate hearth refractory have been assessed by heating samples of calcium aluminates (CA, CA2 & CA6) coupled with aluminosilicate refractory to temperatures representative of the blast furnace hearth (1450°C to 1550°C) in an inert atmosphere over a range of reaction times (4 - 24 hours).

It was found that there was significant reaction between the refractory, CA and CA2 but little reaction with the CA6. The reaction layers formed at the interface between the couples were found to consist of CA2, CA6, corundum, plagioclase and melilite. The formation of a layer with these phases is likely to cause refractory wear due to reduced mechanical strength at highest operating temperatures and by spalling induced by volume changes and changes in thermal expansion characteristics.

From assessment of the kinetics of the system it was found that the aluminosilicate refractory followed the linear rate law for reactions with CA and CA2. Given the lack of reaction of the refractory with CA6 little comment can be made on the kinetics other than they are slow.

**Keywords:** *blast furnace; hearth; refractory; coke ash; calcium aluminates; aluminosilicate; refractory wear; CA ( $\text{CaO} \cdot \text{Al}_2\text{O}_3$ ); CA2 ( $\text{CaO} \cdot 2\text{Al}_2\text{O}_3$ ); CA6 ( $\text{CaO} \cdot 6\text{Al}_2\text{O}_3$ )*

## I. INTRODUCTION

Typically blast furnace hearth refractories are primarily composed of micropore carbon refractory protected by layers of aluminosilicate and alumina-carbon refractories as shown in Figure 1 [1]. These refractory materials may react with coke

ash formed during the dissolution of coke in iron. Coke is composed of carbon and up to 15 mass% oxides [2]. Carbon dissolution of the carbon from the coke into liquid iron can leave an oxide layer at the coke-iron interface. Given that this oxide material in feed coke is approximately 50 mass%  $\text{SiO}_2$ , this layer was expected to be siliceous. However recent studies by Chapman et al [2 -5] have found that coke ash is comprised largely of calcium aluminates.

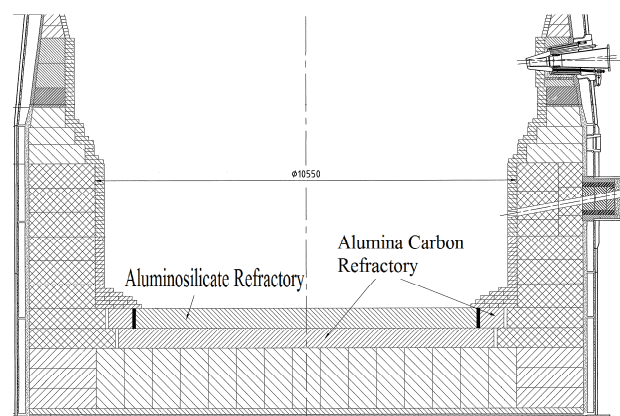


Figure 1. Number 5 blast furnace Port Kembla hearth refractory design [1].

In the hearth, below the iron-slag interface, this material is not dissolved in the slag and is therefore able to settle on the hearth refractories. In this situation it may be expected that the calcium aluminate coke dissolution products could react with the aluminosilicate and alumina-carbon hearth refractories. These reactions may promote hearth wear and reduce the blast furnace campaign life. Understanding the nature of the calcium aluminate refractory reactions are important if blast furnace hearth refractory life is to be optimised. Characterising and understanding these reactions is the subject of this study.

## II. EXPERIMENTAL

The interactions between coke ash and blast furnace hearth refractories were investigated using an aluminosilicate refractory and various synthetic coke ash reaction couples. These reaction couples were heated under a high purity (99.99%) argon atmosphere at temperatures representative of the blast furnace hearth using the experimental configuration outlined in Figure 2. The argon was passed through ascarite,

drierite and then copper turnings at 300°C prior to entering the furnace.

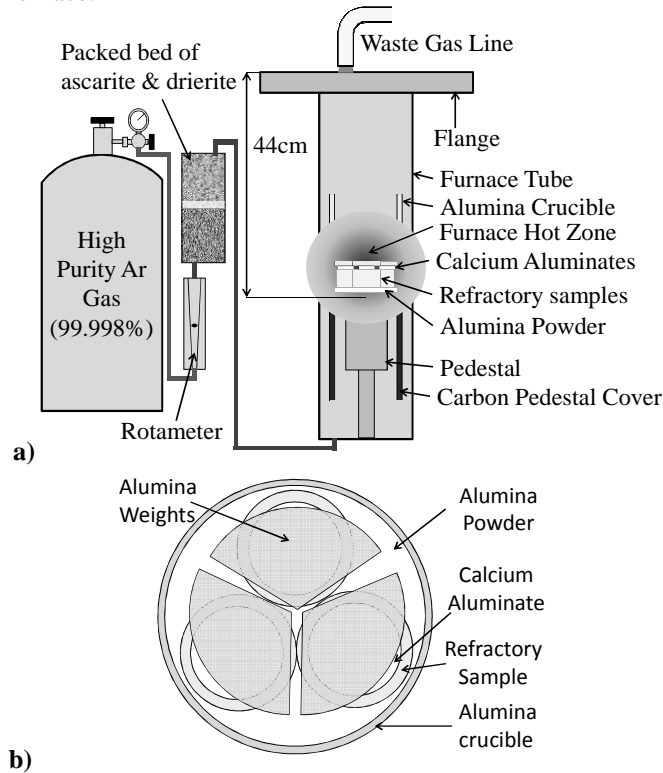


Figure 2. Gas Scrubbing and high temperature furnace experimental setup schematic

The aluminosilicate refractory was tested with each of the calcium aluminates (( $\text{CaO} \cdot \text{Al}_2\text{O}_3$ ,  $\text{CaO} \cdot 2\text{Al}_2\text{O}_3$  and  $\text{CaO} \cdot 6\text{Al}_2\text{O}_3$ ) for reaction times of 4, 8, 12, 18 and 24 hours at 1500°C. Each reaction couple was also tested for 4 hours at 1450°C, 1500°C, 1530°C and 1550°C (with the exception of CA at 1550°C and CA6 at 1530°C). After testing the samples were cooled in the furnace at 5°C min<sup>-1</sup>.

The reaction couples were then mounted and sectioned as shown in Figure 3. The interfaces of these reaction couples and any reaction products were characterised using scanning electron microscopy (SEM) and energy dispersive spectroscopy (EDS).

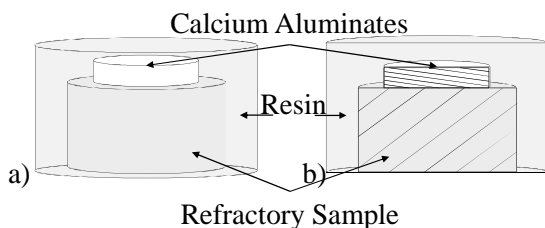


Figure 3. Cold mounted and sectioned reaction couple for SEM analysis

The thickness of the reaction layer at the refractory-aluminate interface was measured using image analysis. An example of a measurement is given in Figure 4. shows an example measurement of the reaction layer thickness using the image analysis software. This measurement was repeated across the

length of the layer 90 times and the average reported as the layer thickness.

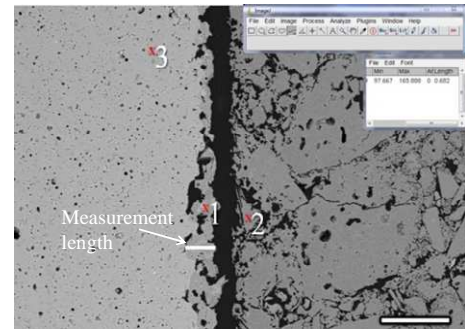


Figure 4. Image Analysis of Aluminosilicte CA reaction couple showing a layer thickness measurement..

#### A. Materials Preparation

Representative samples of the aluminosilicate hearth refractory and synthetic coke ash compositions ( $\text{CaO} \cdot \text{Al}_2\text{O}_3$ ,  $\text{CaO} \cdot 2\text{Al}_2\text{O}_3$  and  $\text{CaO} \cdot 6\text{Al}_2\text{O}_3$ ) were used in this study. The use of synthesised calcium aluminates eliminates the variability typical of industrial coke ash compositions and phase dispersions allowing for much better control of the compositions of the reactants improving the experimental reliability. The method used by Chapman [2] to produce the single phase calcium aluminates was used for this study.

In a study by Drain [6] the aluminosilicate refractory was characterised by taking a number of samples from different locations in the refractory brick as shown in Figure 5. It was found that the microstructure was independent of the position within the refractory brick. No large defects or variations in microstructure (e.g. laminations) were observed throughout the material. The refractory was found to consist of mullite and corundum phases (Table I).

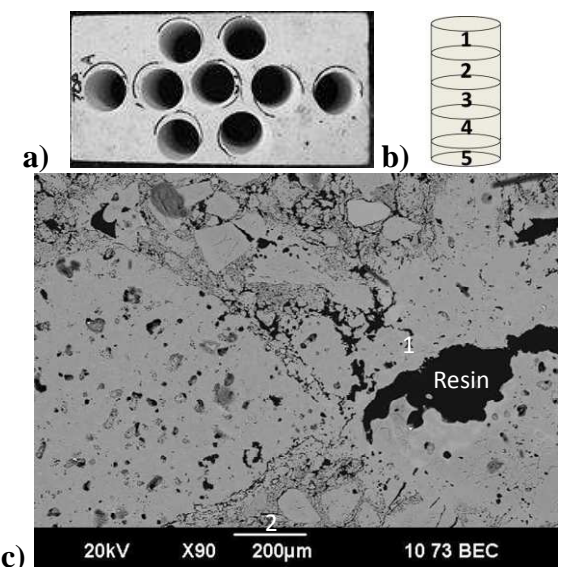


Figure 5. a) Aluminosilicate core samples b) sample positions c) sample microstructure.



TABLE I. ALUMINOSILICATE REFRACTORY EDS SPOT AND AREA ANALYSIS RESULTS

EDS Position	Al <sub>2</sub> O <sub>3</sub> (Mass%)	SiO <sub>2</sub> (Mass%)	FeO (Mass%)	Identified Phase
1	66.7	31.7	1.6	Mullite
2	94.0	6.0		Corundum

The surface of each material was polished to achieve a surface roughness of less than 3µm.

### III. RESULTS AND DISCUSSIONS

For each of the reaction couples tested SEM micrographs were produced as shown in Figure 6.

Selected EDS elemental maps are given in Figure 7. EDS spot analysis compositions at the points indicated in Figure 6 were used to identify the phases at the interface in the reaction couples. These are given in Table II and III.

The reaction phases identified via EDS spot analysis were compared with those predicted by the phase stability diagrams (Figure 8) produced from the MTDATA thermodynamic modelling software [7]. Not all the phases predicted by MTdata were observed in the reaction couples. This is most likely a kinetic effect and not surprising as the couples were not expected to be at equilibrium.

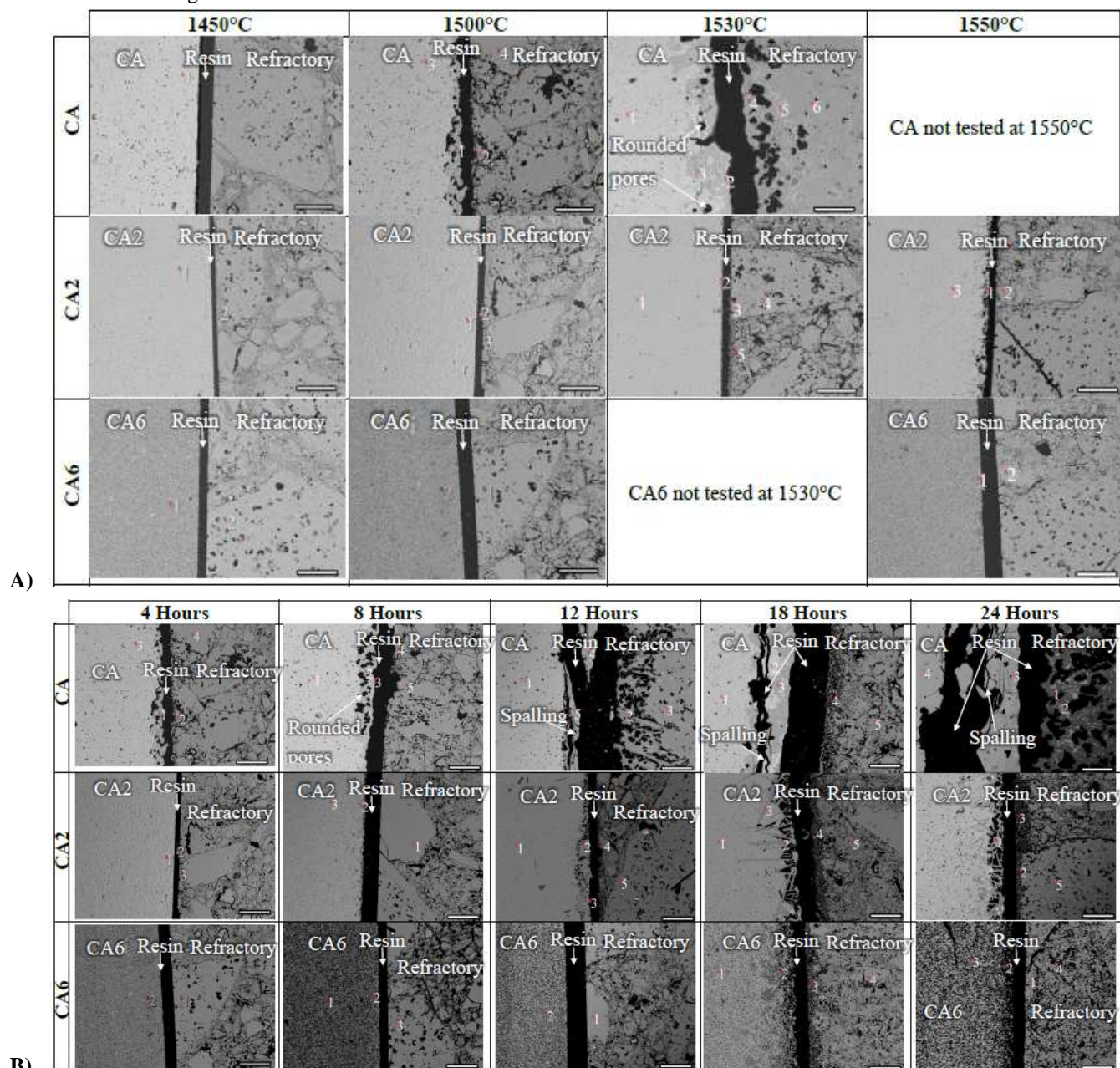


Figure 6. Scanning electron micrographs produced for each reaction couple tested. A) The temperature series 1450-1550°C, B) Time series 4 – 24 hours. Numbered spots represent spot analysis points. Scalebar = 200 µm.

TABLE II. ALUMINOSILICATE REFRACTORY TEMPERATURE SERIES REACTION COUPLES EDS SPOT ANALYSIS RESULTS, AT 4 HOURS REACTION TIME. UNITS = MASS%. NOTE: ONLY THE 1450°C, 1500°C AND 1550°C DATA IS SHOWN

	Spot No.	1450°C				1500°C				1550°C			
		Al <sub>2</sub> O <sub>3</sub>	CaO	SiO <sub>2</sub>	Phase	Al <sub>2</sub> O <sub>3</sub>	CaO	SiO <sub>2</sub>	Phase	Al <sub>2</sub> O <sub>3</sub>	CaO	SiO <sub>2</sub>	Phase
CA	1	64.6	35.4		CA	77.2	15.4	7.4	Hibonite (CaAl <sub>12</sub> O <sub>19</sub> )	CA not tested at 1550°C			
	2					63.3	4.6	32.1	Mullite				
	3					64.5	35.5		CA				
	4					67.5	1.75	30.8	Mullite				
CA2	1	78.8	21.2		CA2	77.9	22.12		CA2	91.6	8.4		CA6
	2	87.9		12.0	Corundum	100			Alumina Grain	75.2		24.8	Mullite
	3					67.0		32.9	Mullite	78.0	22.0		CA2
CA6	1	90.7	9.3		CA6	76.7		23.3	Mullite Grain	90.4	9.6		CA6
	2	73.8		26.2	Mullite Grain	91.0	9.0		CA6	73.1		26.9	Mullite

TABLE III. ALUMINOSILICATE REFRACTORY TIME SERIES REACTION COUPLES EDS SPOT ANALYSIS RESULTS AT 1500°C REACTION TEMPERATURE.

	Spot No.	4 Hours				8 Hours				12 Hours			
		Al <sub>2</sub> O <sub>3</sub>	CaO	SiO <sub>2</sub>	Phase	Al <sub>2</sub> O <sub>3</sub>	CaO	SiO <sub>2</sub>	Phase	Al <sub>2</sub> O <sub>3</sub>	CaO	SiO <sub>2</sub>	Phase
CA	1	77.2	15.4	7.4	Hibonite	65.3	34.7		CA	63.5	36.5		CA
	2	63.3	4.6	32.1	Mullite	73.8	26.2		CA2/ Grossite	76.8	5.9	17.3	Corundum
	3	64.5	35.53		CA	38.2	22.5	39.3	Gehlenite (Melilite)	71.3		28.7	Mullite
	4	67.5	1.8	30.8	Mullite	83.4	11.3	5.3	Corundum	78.8	21.2		CA2
	5					65.4	33.1	1.6	Mullite	79.0	21.0		CA2
CA2	1	77.9	22.1		CA2	57.8		42.2	Mullite	78.13	21.9		CA2
	2	100			Alumina Grain	91.9	8.2		CA6	89.01	2.4	8.6	Corundum
	3	67.1		32.9	Mullite	77.8	22.2		CA2	61.81	12.1	26.1	CA2 / Hibonite
	4									75.55	24.4		Mullite
	5									70.73	29.3		Mullite
CA6	1	76.7		23.3	Mullite Grain	93.3	6.7		CA6 / corundum	68.2	0.4	31.4	Mullite
	2	91.0	9.0		CA6	91.2	8.8		CA6 / corundum	89.5	8.5	2.0	Corundum
	3					77.1		23.0	Mullite				
	Spot No.	18 Hours				24 Hours							
		Al <sub>2</sub> O <sub>3</sub>	CaO	SiO <sub>2</sub>	Phase	Al <sub>2</sub> O <sub>3</sub>	CaO	SiO <sub>2</sub>	Phase				
CA	1	67.8	32.2		CA	100.0			Corundum				
	2	67.8	32.2		CA	37.7	18.3	44.0	Anorthite (plagioclase)				
	3	79.5	20.5		CA2	80.3	19.6	0.1	CA2/ Grossite				
	4	100.0			corundum	66.8	33.1	0.1	CA				
	5	67.8		32.2	Mullite								
CA2	1	79.5	20.5		CA2	91.4	7.8	0.8	Corundum / CA6				
	2	92.3	7.7		CA6	100.0	0.0		Corundum				
	3	92.3	7.7		CA6	100.0	0.0		Corundum				
	4	100.00			Corundum	59.5	1.2	39.3	Mullite				
	5	75.6		24.4	Mullite	74.8	0.9	24.3	Mullite				
CA6	1	91.4	8.6		CA6	75		25	Mullite				
	2	100			Corundum	42.1	16.9	41.0	Corundum				
	3	100			Corundum	85.4	10.6	4.0	Corundum				
	4	73.7		26.3	Mullite	72.3	0.1	27.6	Mullite				

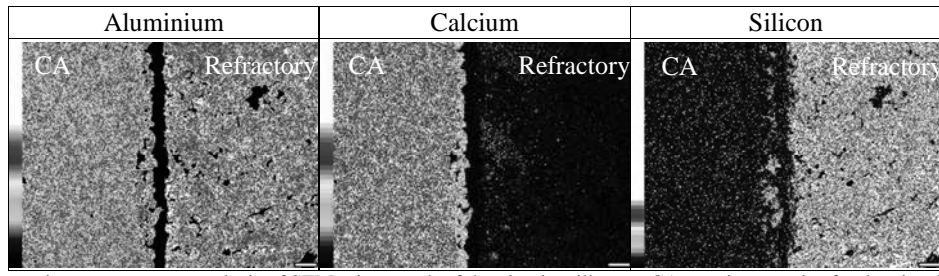
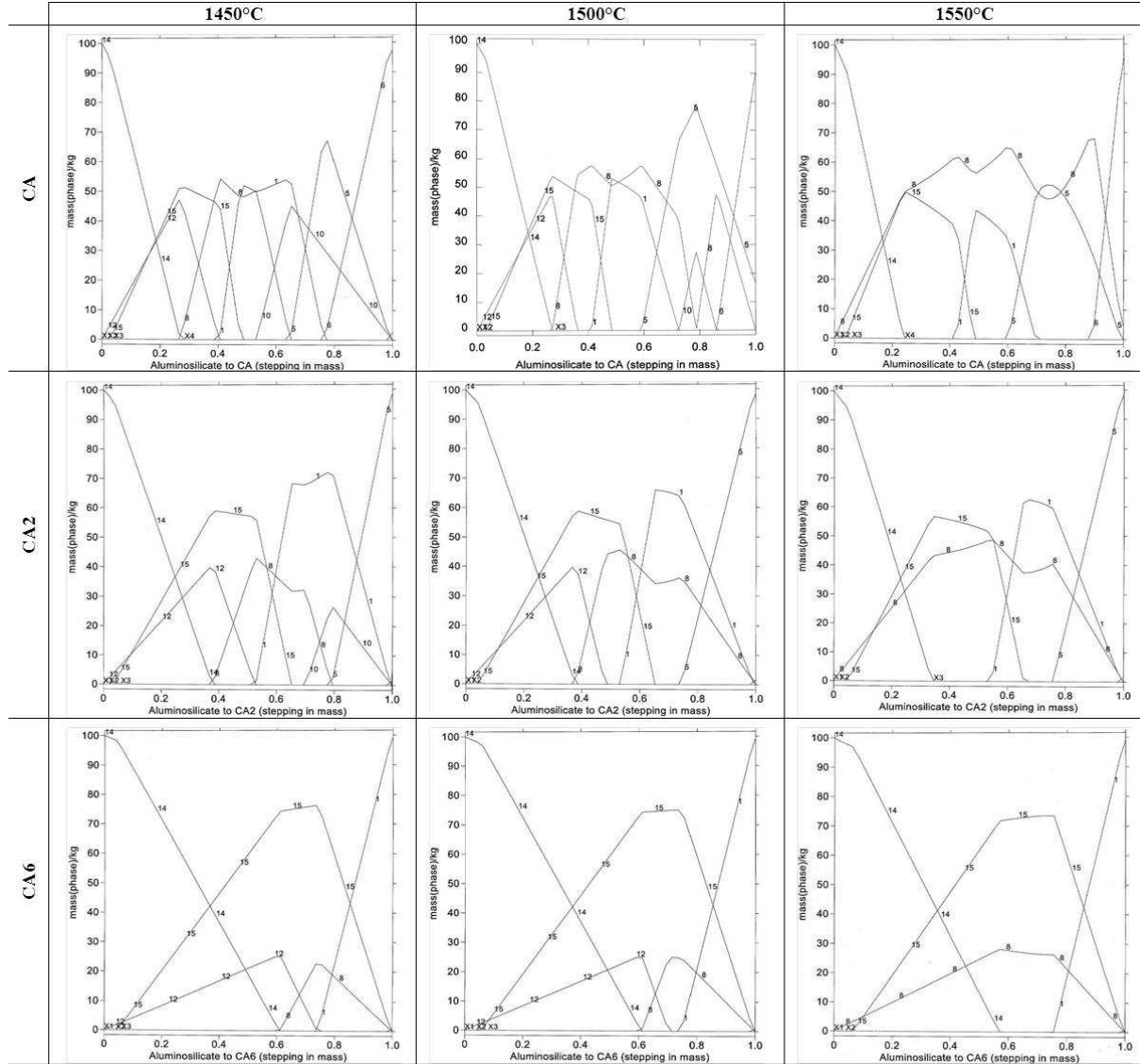


Figure 7. Energy dispersive spectroscopy analysis of SEM micrograph of the aluminosilicate – CA reaction couple after heating for 4 hours at 1500°C. Scalebar = 100 µm.



1 = CA6, 5 = CA2, 6 = CA, 7 = C12A7, 8 = Liquid oxide, 10 = Melilite, 12 = Plagioclase H, 13 = Spinel, 14 = Mullite, 15 = Corundum

Figure 8. Phase stability diagrams showing the mass of phases present at different aluminosilicate CAx mass ratios for the reaction temperatures 1450°C- 1550°C using the MTDat [7].

The time dependency for the formation of the various phases predicted by the phase stability diagrams (Figure 8) was tested by comparing phases formed at different reaction times with the equilibrium phases predicted in Figure 8. It was found that some phases take a significant amount of time to form. The formation of CA6, melilite, plagioclase and corundum were all

found to be time dependant. Each of these phases were only observed at longer reaction times e.g. 8 hours for melilite and 24 hours for plagioclase.

The formation of some phases was also found to be temperature dependent. The formation of CA2 and melilite in

particular was found to be temperature dependent; both were only observed after 4 hours above 1530°C reaction temperature. However each of these phases were predicted to be thermodynamically stable at lower temperatures in Figure 8. This is most likely due the higher reaction rates at higher temperatures. The rate of reaction for most high temperature refractory reaction processes follow simple kinetics where the rate is in part proportional to a rate constant  $k$  [8] . This  $k$  may be representative of mass transfer or chemical reaction control kinetics. Temperature effects on  $k$  can be predicted by the Arrhenius equation (1) [8].

$$k = k_0 e^{\left(\frac{-Q}{RT}\right)} \quad (1) [8]$$

where  $k_0$  is a pre-exponential constant,  $Q$  an activation energy,  $R$  is the gas constant and  $T$  the thermodynamic temperature.

From equation 1 it can be seen that  $k$  has an exponential relationship with temperature, whereby increasing temperature increases  $k$  and hence increases the rate of reaction.

In reviewing Figure 8 it can be seen that for all the reaction couple systems studied there is the potential for liquid phase formation, particularly in the higher CaO calcium aluminates and high temperature reaction couples. Given the reaction

analysis is post experiment at ambient temperatures no liquid oxide was observed directly. Indirect evidence of liquid formation could be local densification of the reaction couple, pore penetration by the liquid, curvature of phases formed and/ or the surrounding pores and compositions of phases representative of what would be expected of a liquid at the experimental temperature. There is some evidence of these in Figure 6. There are rounded or curved pores that may indicate that a liquid has been present. Though this is not definitive as such pores can be caused by solid state reaction that causes volume change. There are also compositions corresponding to phases of what might be expected to have been a liquid oxide (plagioclase and melilite in Table III) at the experimental temperature.

The liquid oxide phase, as predicted by MTdata [7] has a composition of approximately 35 mass%  $\text{SiO}_2$ , 32 mass%  $\text{Al}_2\text{O}_3$  and 33 mass%  $\text{CaO}$ . This composition could readily solidify to form melilite and plagioclase. Since both these were identified in Table III this indicates a liquid oxide phase may have been present at the experimental temperature.

#### A. Aluminosilicate Refractory Reaction Kinetics

Reaction layer thickness measurements were taken using image analysis of the micrographs in Figure 6.

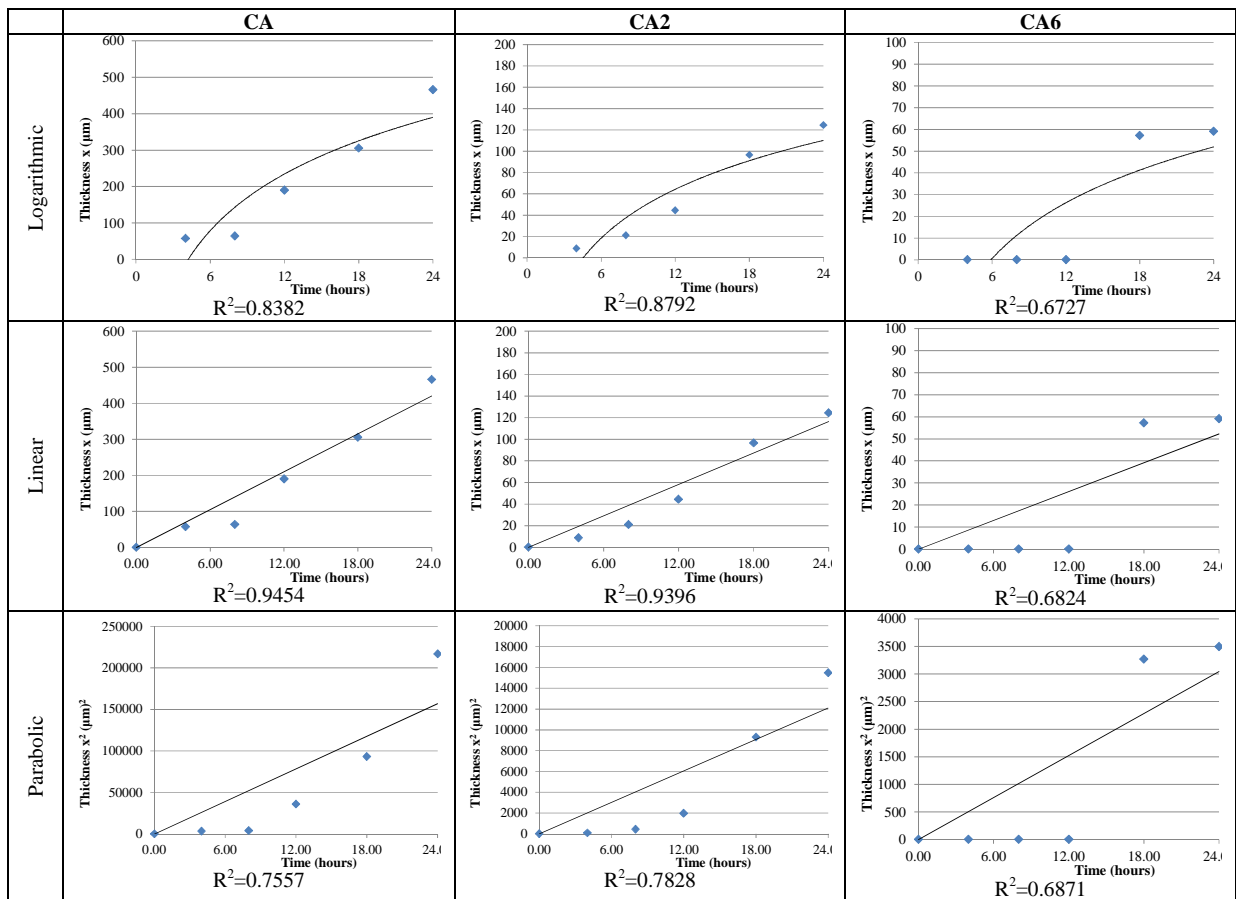


Figure 9: Aluminosilicate – Calcium aluminate reaction couples thickness of reaction layer by time. The solid line represents the best fit to the respective rate law being tested.



These data were used to test for linear, parabolic and logarithmic kinetic behaviour (equations 2 – 4 respectively) [9, 10] between the aluminosilicate refractory and calcium aluminates and are given in Figure 9.

$$x = k_{lin}t + A \quad (2) [9, 10]$$

$$x^2 = 2k_{par}t + B \quad (3) [9, 10]$$

$$x = k_{log} \log t + C \quad (4) [9, 10]$$

where  $x$  = reaction layer thickness  
 $k$  = respective rate constant  
 $t$  = time  
 $A, B$  &  $C$  are constants

The  $R^2$  values were used as the discriminating parameter for deciding best fit in Figure 9. The  $R^2$  values of 0.9454 and 0.9396 for the CA and CA2 reaction couples indicates a good fit of the experimental data to the regression line for the linear rate law (equation 4) [9, 10]. The CA6 reaction couples had poor fits to the logarithmic, linear and parabolic rate laws with  $R^2$  values of 0.672, 0.682 and 0.687 respectively. The poor fit is most likely due to the very small reaction layer observed and small data set caused by the reaction layer only forming at the longer reaction times.

Linear reaction kinetics in refractory systems occur when the reaction layers have high porosity, cracking, spalling or consist of a liquid phase. These defects prevent the reaction (product) layer from slowing the reaction kinetics. The CA and CA2 reaction couples were observed to form reaction layers with high porosity at temperatures of 1500°C or greater (Figure 6). This reaction mechanism is consistent with phenomena observed in the micrographs shown in Figure 6. In this Figure there is evidence of spalling and cracking of the reaction layer at reaction times >12 hours. Also as previously discussed there is evidence that a liquid may have been present at the experimental temperature.

There is a general trend of increasing reaction layer thickness with greater  $Ca^{2+}$  content of the calcium aluminate. This indicates that  $Ca^{2+}$  is playing a key role in the reaction kinetics. Though not explored in this study, it may be expected that there would be a greater thermodynamic driving force for reaction or calcium transfer in the higher  $Ca^{2+}$  calcium aluminates.

#### B. Influence of Reaction Products Properties on Refractory Degradation

The possible formation of the liquid oxide phase may accelerate the rate of refractory loss via removal of the liquid phase and reduce wear resistance of the high porosity region remaining at the refractory surface. Table IV provides the unit cell volume, density and thermal expansion coefficients of selected solid phases observed to be present in the reaction layer.

It can be seen from Table IV that the mullite thermal expansion coefficient is significantly different to the reaction product phases ( $6 \times 10^{-6}/K$  compared to  $1.6 \times 10^{-6}/K$  and  $26 \times 10^{-6}/K$ ). This difference will increase the susceptibility of the refractories to degradation by thermal spalling when exposed to cyclic temperatures.

TABLE IV. UNIT CELL VOLUME, DENSITY AND THERMAL EXPANSION COEFFICIENT OF COKE ASH AND HEARTH REFRACTORY MINERALS [11 - 16]

Phase	Unit Cell Volume ( $\text{\AA}^3$ )	Density ( $\text{g/cm}^3$ )	$\alpha$ ( $10^{-6}/K$ )
CA ( $\text{CaO} \cdot \text{Al}_2\text{O}_3$ )	1069.4	2.92	~26
CA2 ( $\text{CaO} \cdot 2 \text{Al}_2\text{O}_3$ )	297.7	2.9	~24
CA6 ( $\text{CaO} \cdot 6 \text{Al}_2\text{O}_3$ )	588.1	3.77	~21
Corundum ( $\text{Al}_2\text{O}_3$ )	84.9	3.99	19
Plagioclase ( $\text{CaO} \cdot \text{Al}_2\text{O}_3 \cdot 2\text{SiO}_2$ )	697.64	2.76	1.6 – 2.38
Melilite ( $2\text{CaO} \cdot \text{Al}_2\text{O}_3 \cdot \text{SiO}_2$ )	299.05	2.98	~7.2
Mullite ( $3 \text{Al}_2\text{O}_3 \cdot 2\text{SiO}_2$ )	169.7	3.08 – 3.17	~6

Volume changes due to the formation of reaction products can produce stresses and subsequent spalling of the refractory materials. There is also evidence of this in Figure 6. The increase in unit cell volume in the reaction layer is between 75% (formation of CA2 in the refractory) and 411% (formation of Plagioclase).

The calcium aluminates, plagioclase ( $\text{CaO} \cdot \text{Al}_2\text{O}_3 \cdot 2\text{SiO}_2$ ) and melilite ( $2\text{CaO} \cdot \text{Al}_2\text{O}_3 \cdot \text{SiO}_2$ ) all have lower liquidus temperatures than the refractory phases (mullite and corundum). The calcium aluminates soften between 1500°C and 1600°C, which is within the range of hearth temperatures (1450°C - 1550°C). Therefore the reaction layer is likely to have a lower resistance to mechanical wear and deformation than the refractories.

#### C. Refractory – Coke ash reaction kinetics in the blast furnace hearth

The experimental methodology used for this study represents the situation in the hearth in which coke ash comes into contact with the hearth refractory without any molten iron present at the interface. Due to the non-wetting behaviour of iron melts with calcium aluminates [17] and aluminosilicates [18] the absence of an iron melt at the interface is believed to be a good assumption for localised conditions within the hearth. The molten iron in the blast furnace hearth also contains [Si] up to 0.9% at 1550°C in some cases [19]. This [Si] may react with the calcium aluminates and refractory and assist in the formation of low melting point phases such as plagioclase and melilite. The experimental setup used did not simulate the cyclical coke bed float/sink conditions that can occur in a blast furnace hearth [20]. These cyclical conditions would increase

the removal rate of any reaction products via high iron flows or coke bed movement and subsequently increase the wear rate.

### CONCLUSIONS

In a study of blast furnace hearth aluminosilicate refractory reactions with CA, CA2 and CA6 coke ash minerals it was found that the kinetics of the refractory reaction with the CA and CA2 follow the linear rate law. This is typical of a material that forms a non-protective reaction layer with high porosity and forms liquid phase reaction products. Given the limited amount data obtained for the CA6- aluminosilicate couples and the poor fit to the data obtained, little comment can be made on its kinetic behavior other than the reaction was slow.

The rate of reaction was observed to be dependent on temperature and the CaO composition of the synthetic coke ash. It was not clear whether a liquid formed during reaction of the refractory- CAx couples. Thermodynamic analysis indicated this was possible and there was some micro-structural and composition evidence that indicated it may have occurred.

The combined effects of the volume and thermal expansion changes of the reaction products formed are likely to increase the susceptibility of the blast furnace hearth refractory to spalling during furnace operation. This is significant as spalling releases fresh material for further reaction/degradation with the coke ash.

### REFERENCES

- [1] Cook, S.R., 2007, *No.5 Blast Furnace – 2007 Reline, Furnace, Refractories, General Arrangement*, BlueScope Steel drawing number 460373, Port Kembla, Australia.
- [2] Chapman, M.W., 2009, *Insoluble oxide product formation and its effect on coke dissolution in liquid iron*, PhD thesis, University of Wollongong, Wollongong, Australia
- [3] Chapman, M.W., Monaghan, B. J., Nightingale, S. A., Nightingale, R. J. & Mathieson, J.G 2008, 'Formation of a Mineral Layer during Coke Dissolution into liquid Iron and its influence on the Kinetics of Coke Dissolution Rate', *Metallurgical and Materials Transactions B*, vol. 39, no.3, pp. 418-430.
- [4] Chapman, M.W., Monaghan, B.J., Nightingale, S.A., Mathieson, J.G. & Nightingale, R.J., 2007, *Observations of the Mineral Matter Material Present at the Coke/Iron Interface During Coke Dissolution into Iron*. ISIJ International, vol.47, no.7, pp. 973-981.
- [5] Chapman, M. W., Monaghan, B. J., Nightingale, S. A., Mathieson, J. G. & Nightingale, R. J. 2011, *The effect of sulfur concentration in liquid iron on mineral layer formation during coke dissolution*, *Metallurgical and Materials Transactions B: Process Metallurgy and Materials Processing Science*, vol. 42, no. 4, pp. 642-651.
- [6] Drain, P.B., 2010, *Blast Furnace Hearth Refractory and Coke Ash Interactions*, Honours thesis, University of Wollongong, Wollongong Australia
- [7] Davies, H., Dinsdale, A.T, Gisby, J.A., Robertson, J.A.J. & Martin, S.M. , 2002, *MTDATA– Thermodynamic and Phase Equilibrium Software from the National Physical Laboratory*, Calphad, 26 (2), 229-271
- [8] Kofstad, P., 1966, *High Temperature Oxidation of Metals*, John Wiley & Sons, London.
- [9] Khanna, A. S., 2002, *Introduction to High Temperature Oxidation and Corrosion*, ASM International, USA. pp. 9 – 11.
- [10] Poirier, D.R., & Geiger, G.H., 1994, *Transport Phenomena In Materials Processing*, TMS, Warrendale, PA, pp. 444-93
- [11] Carter, C.B., Norton, M., 2007, *Ceramic Materials Science and Engineering*, Springer
- [12] Kowalski, M., Spencer, P.J. & Neuschütz, D. 1995, in *Slag Atlas*, VDE (VDEh), ed., VerlagStahleisen GmbH, Dusseldorf, Germany, pp. 39.
- [13] Levin, E.M., Robbins, C.R., & McMurdie, H.F., 1964, *Phase Diagrams For Ceramists*, The American Ceramic Society, Columbus, Ohio
- [14] Hofmeister, A. M., 2004, *Physical properties of calcium aluminates from vibrational spectroscopy*, *Geochimica et Cosmochimica Acta*, Vol. 68, No. 22, pp. 4721-4726,
- [15] (eds.) Lankford, W.T., Samways, N.L., Craven, R.F. & McGannon, H.E., 1985, *Making, Shaping and Treating of Steel*, Herbeck & Held, Pittsburg, p.367-441.
- [16] Tribaudino, M., Angel, R. J., Cámara, F., Nestola, F., Pasqual, D. & Margiolaki, I., 2010, *Thermal Expansion of Plagioclase feldspars*, *Contributions to Mineralogy and Petrology*, Vol. 160, No. 6, pp.899-908
- [17] Monaghan, B.J., Chapman, M.W. & Nightingale, S.A., 2010, *Liquid Iron Wetting of Calcium Aluminates*, *ISIJ International*, vol. 50, no.11, pp. 1707-1712.
- [18] Kapilashrami, E., Sahajwalla, V. & Seetharaman, S., 2004, *Investigation of the Wetting Characteristics of Liquid Iron on Mullite by Sessile Drop Technique*, *ISIJ International*, vol. 44, no.4, pp. 653-659.
- [19] Kequin, M. I., 1992, *Reduction and Re-oxidation of Silicon in the Blast Furnace*, *Chin. J. Met. Sci. Tech.*, vol. 8, pp. 435-439
- [20] Nightingale, R.J., 2000, *The development and Application of Hearth Voidage Estimation and Deadman Cleanliness Index for the Control of Blast Furnace Hearth Operation*, PhD thesis, University of Wollongong, Wollongong, Australia